

Kinetics of the pyrolysis of *n*-butane

JOHN TOROK¹ AND SAMUEL SANDLER

*Department of Chemical Engineering and Applied Chemistry,
University of Toronto, Toronto, Ontario*

Received June 19, 1969

The thermal decomposition of *n*-butane was investigated at temperatures ranging from 330 to 420 °C. This extension of the temperature range for such studies was made possible by the use of a highly sensitive analytical system, consisting of a gas-liquid chromatograph equipped with a hydrogen-flame-ionization detector which permitted the determination of the major products of the reaction at reactant conversions as low as 0.0002%. At temperatures below 400 °C the reaction order was both temperature and pressure dependent, a lower order, approaching 0.5, being favored at lower temperatures and higher pressures. The contribution to the reaction mechanism of a chain-termination step consisting of the combination of 2 secondary butyl radicals explains the observed phenomena.

Canadian Journal of Chemistry, 47, 3863 (1969)

Introduction

Recent investigators of the thermal decomposition of *n*-butane (1, 2) have been concerned with the reaction in the temperature range of 420–590 °C. On the other hand, studies of the sensitized decomposition have generally been conducted at temperatures below 340 °C. Thus, though this reaction has been studied extensively, no thorough investigation at the intermediate temperatures had been made prior to the present one.

Although the pyrolysis of *n*-butane is one of the better understood free-radical chain reactions, it is still necessary to point out, as in a recent publication by the present authors (3), that the main chain-ending step of this reaction at temperatures above 420 °C is still obscure. The present work is mainly concerned with the elucidation of the chain-termination mechanism at temperatures below 420 °C.

Purnell and Quinn (1) have made the most significant contribution of the last 2 decades to the clarification of the mechanism of this reaction. They identified most of the products, including the minor ones, thoroughly investigated the temperature and pressure dependence of the distribution of the major products, and determined that the decomposition of the ethyl radical was in its pressure-dependent region.

Due to the large apparent activation energy for this reaction (about 63 kcal/mole) the reaction rate rapidly decreases with a decrease in reaction temperature. Thus, this extension of the tem-

perature range over which the pyrolysis of *n*-butane could be studied required, and was made possible only as a result of, the development of a highly sensitive analytical system. Gas-liquid chromatography in conjunction with hydrogen-flame-ionization detection was used to determine the major products of the reaction at conversions as low as 0.0002%.

Experimental

A conventional static reaction system was used. The reactor and auxiliary glass vessels were connected to a vacuum system capable of maintaining pressures near 10^{-5} Torr.

Phillips Petroleum Co. Research Grade *n*-butane was treated to remove traces of isobutane, propane, and butene impurities. It was first adsorbed at ambient temperature on Linde molecular sieve, Type 5A, and the unadsorbed vapors containing isobutane were pumped off and discarded. The adsorbed *n*-butane and propane were then desorbed at 170 °C, a temperature at which olefins would still be retained, and passed through a bed of Type 4A molecular sieve at ambient temperature to remove propane. The reactant now contained no hydrocarbon impurities detectable by sensitive gas-liquid chromatography.

Traces of oxygen and other fixed gases were carefully removed by prolonged degassing of the condensed reactant at -107 °C. This was followed by repeatedly bubbling the gas through a 100 mm column of aluminum amalgam (4) to further lower the oxygen content to a negligible value.

The reaction bulb was housed and heated in an electronically controlled 3 section oven capable of maintaining a constant temperature along the length of the reactor, within ± 0.3 °C. Two 80 ml quartz reaction vessels were used. The bodies of the reactors were cylindrical, 2.5 cm in diameter and 21 cm in length. Each contained a coaxial thermowell terminating at the center of the reactor. One of the reactors was unpacked and had a surface-to-volume ratio (s/v) of 2.1 cm^{-1} . The other

¹Present address: Norton Research Corporation, Chippawa, Ontario.

was packed with enough quartz tubing to yield a value of s/v of 7.7 cm^{-1} . The effect of using reaction times between 15 s and 2 h, and pressures in the range 16 to 600 mm Hg, could be usefully investigated with this apparatus.

At any desired stage of the reaction, the reactor contents were expanded into a previously evacuated bulb. Subsequently, the bulb contents were compressed over mercury and a portion transferred into the 2 ml sample loop of a Varian-Aerograph Model 600-D gas chromatograph equipped with a high sensitivity hydrogen-flame-ionization detector.

The gas-liquid chromatographic analysis was limited to the 4 major hydrocarbon products of the reaction, since it was not possible to obtain quantitatively significant quantities of the minor products at the low conversion conditions of this study. Furthermore, since a hydrogen-flame-ionization detector was needed at its ultimate sensitivity to detect the major products, product hydrogen could not be detected. Three identical column trains were prepared. Each train contained a 25 ft long, 0.25 in. o.d. copper tube column packed with 60-80 mesh Chromosorb P acid-washed fire brick coated with 29% by weight of dimethylsulfolane (DMS). To this was attached a 6 in. column packed with 60-80 mesh Chromosorb W fire brick coated with 15% by weight of Carbowax 20M. The purpose of the latter was to hold back any DMS tending to bleed from the first column.

The 3 column trains were connected to a common carrier-gas source and any one of them could be connected to the inlet of the hydrogen-flame-ionization detector. Following the elution of methane, ethane, ethylene, and propylene, respectively, from one column, another was connected to the detector for the next analysis. This procedure reduced analysis time and eliminated the necessity for burning excessive amounts of the unreacted butane in the detector. Due to the large sample size required to obtain measurable quantities of reaction products, the column had to be overloaded insofar as *n*-butane was concerned. However, this did not affect the reaction product peaks eluted ahead of *n*-butane, and the latter could be purged from the column to air while one of the other columns was being used for the analysis of another sample.

The analysis for *n*-butane itself was neither feasible nor required, so long as the sample size injected was reproducible and the same sample loop was used for calibration. The calibration was performed on samples of known and very low concentrations of the major hydrocarbon reaction products. Since conversions were always extremely low, reaction rates could be calculated directly from a carbon balance based on the product analysis, assuming that all significant carbon containing products had been determined and that the conversion-time relationship was linear in the region investigated.

Results

The poor reproducibility of the results obtained at temperatures below approximately 380°C was a major problem in this investigation. Various cleaning and coating procedures (5) served only to enhance this problem. Clean reac-

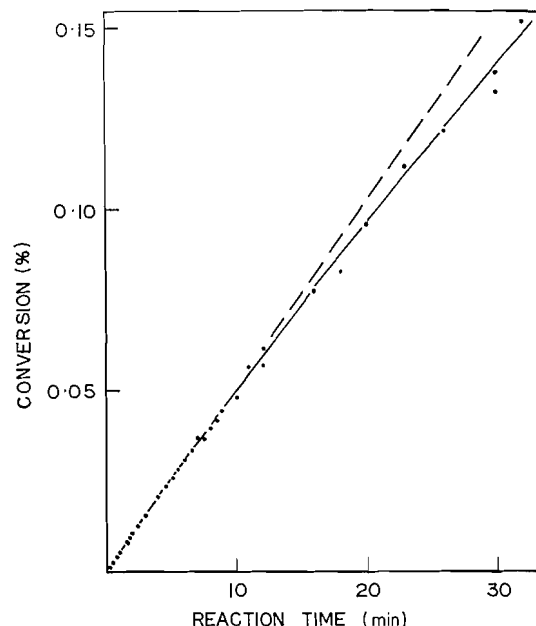


FIG. 1. Reactant conversion as a function of reaction time at 393°C and 200 mm Hg.

tors, freshly fabricated by the glass blower but otherwise untreated, gave the most reproducible results and were used for all final runs.

Figure 1 demonstrates the effect of residence time on conversion at 393°C and 200 mm Hg pressure. The following points may be noted from this figure. (i) The reaction has no observable induction period. This coincides with the observation of Purnell and Quinn (1), but is not consistent with the findings of Sagert and Laidler (2), who observed a short induction period. (ii) After an initial period of several minutes, corresponding to a conversion of less than 0.05%, the reaction rate decreases slightly with reaction time. The broken line is the extension of the initial linear portion of the curve.

At conversions rising to 0.15% product selectivities (defined as moles of product/100 moles of butane decomposed) were found to be independent of conversion.

Figure 2 demonstrates as well the independence of the product selectivities of the reaction pressure at a temperature of 370°C . It is also apparent that the selectivities for methane and propylene on the one hand, and ethane and ethylene on the other, are equivalent.

Several runs were conducted at temperatures

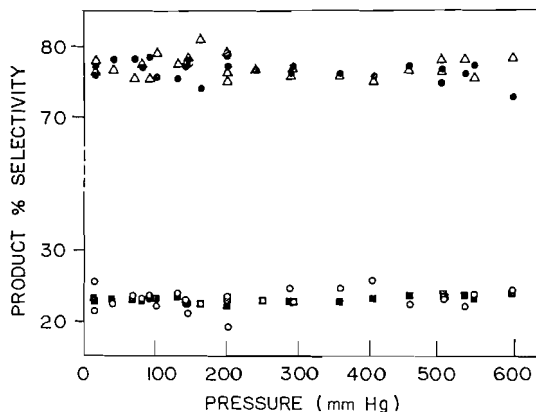


FIG. 2. Product selectivity as a function of reaction pressure at 370 °C. Reaction time range 8–25 min. Δ , methane; \blacksquare , ethane; \circ , ethylene; \bullet , propylene.

above 420 °C to establish some connection with the work of previous investigators. Product selectivities in this temperature range were quite comparable to those obtained by Purnell and Quinn (1). An Arrhenius-type plot of the product selectivities is given in Fig. 3. The slope and position of the line drawn were calculated by the method of least squares and correspond to the equation

$$[I] \quad \frac{[C_2H_4] + [C_2H_6]}{[CH_4] + [C_3H_6]} = 1.8 \exp(-2300/RT)$$

This is comparable with the result obtained by Purnell and Quinn as expressed in the equation

$$\frac{[C_2H_4] + [C_2H_6]}{2[CH_4]} = 1.3 \exp(-2000/RT)$$

Overall Reaction Order

The temperature and pressure dependence of the overall order were thoroughly investigated. At temperatures above 410 °C, the order was found to be both temperature and pressure independent and approximately 1.5.

A log-log plot of the relative rate of pyrolysis at 370 °C against reaction pressure is given in Fig. 4. In this plot the rates are measured relative to the reaction rate at the reference pressure of 194 mm Hg. Every second run was conducted at the reference pressure, while intermediate runs were executed at randomly selected pressures ranging from 16 to 620 mm Hg. The relative rate in Fig. 4, is defined as the rate of reaction at the specified pressure divided by the rate of the succeeding reaction conducted at 194 mm Hg. This treatment of the experimental data was necessary since the results of successive runs at temperatures below 380 °C were much more reproducible than those of runs further separated in time. Points in Fig. 4 were fitted with both linear and curvilinear regressions. A statistical analysis of the 2 regressions indicated that the

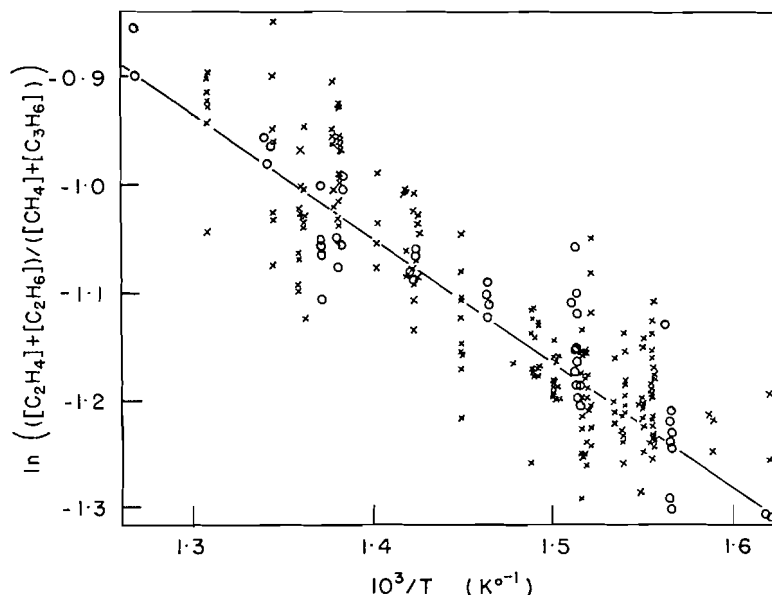


FIG. 3. Arrhenius plot for product selectivities. \circ , packed reactor; \times , unpacked reactor.

departure from the linear regression is significant. The slope of a $\log(\text{rate})$ vs. $\log(\text{pressure})$ curve (at constant temperature) is equivalent to the overall order of reaction. Thus, at 370 °C, the overall reaction order is in its pressure dependent region, a higher order being favored at lower pressures.

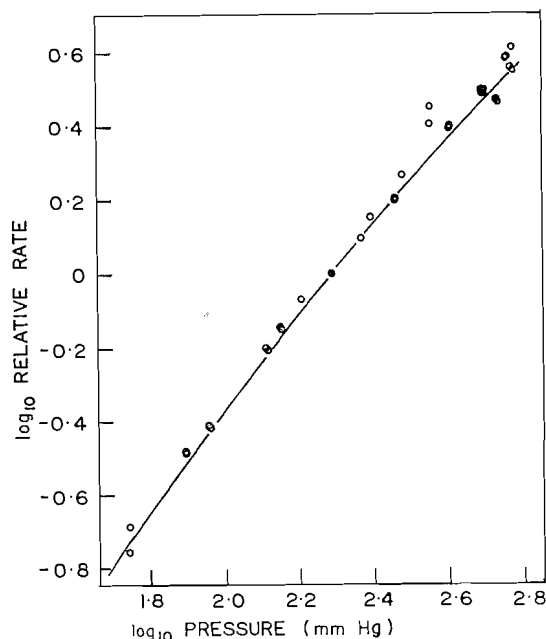


FIG. 4. Logarithm of relative rate as a function of the logarithm of the pressure for the pyrolysis at 370 °C. (Relative rate is defined as the reaction rate at the specified pressure divided by the reaction rate at 194 mm Hg pressure.)

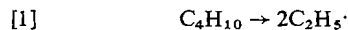
Figure 5 demonstrates the variation of reaction order with temperature. At each temperature, successive runs were conducted at reaction pressures alternating between 94 and 200 mm Hg. From the rates of successive pairs of runs, a reaction order was calculated and plotted against temperature. The differences in the results obtained with packed and unpacked reactors were not significant. The broken line in the figure is a third-degree polynomial least squares fit of all the points. The solid curve is calculated and is described later.

A plot of the natural logarithm of the reaction rate as a function of the reciprocal of the reaction temperature for runs in the unpacked reactor is given in Fig. 6. The upper line is a linear regression for runs at 200 mm Hg, the lower line for runs at 94 mm Hg reaction pressure. The activation energies calculated from the slopes of these regressions are 63.5 and 60.3 kcal/mole, respectively.

Discussion

In a previous publication (3), the authors proposed the following mechanism for this pyrolysis at temperatures above 410 °C.

Initiation



Propagation

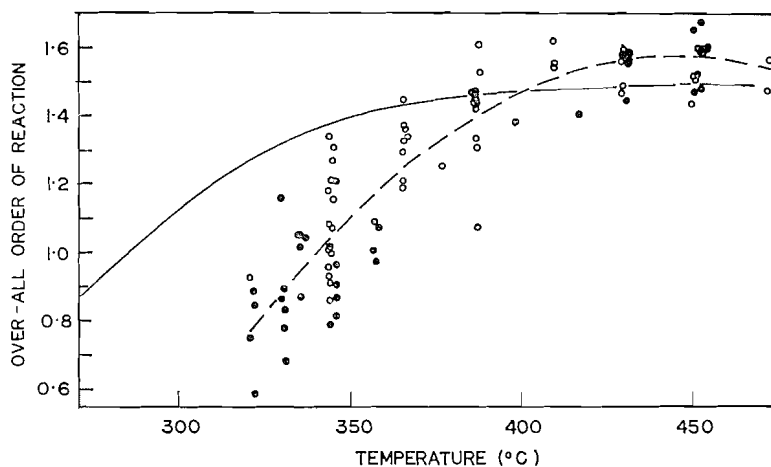
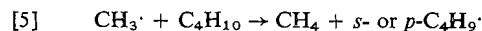
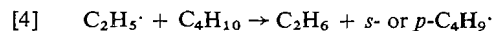
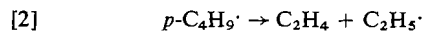


FIG. 5. Variation of overall reaction order with temperature. —, theoretical curve; ---, 3rd degree polynomial fit to data; ○, packed reactor; ●, unpacked reactor.

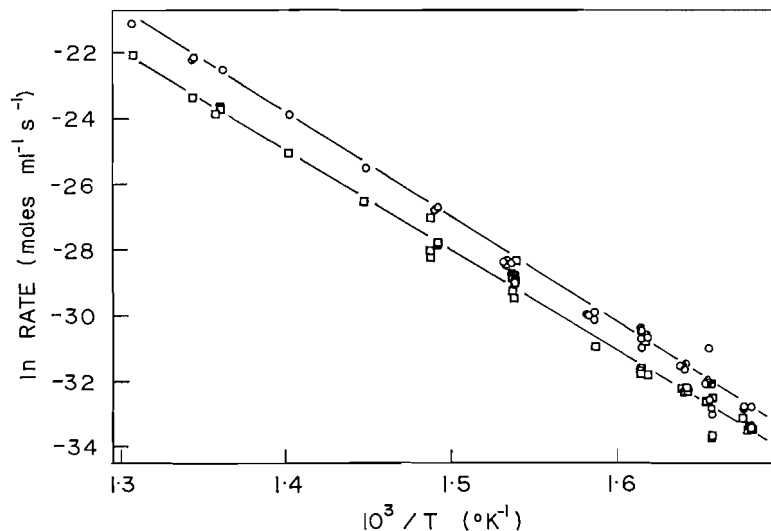
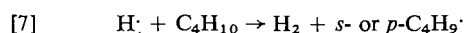
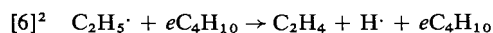


FIG. 6. Natural logarithm of reaction rate as a function of reciprocal temperature for unpacked reactor. Reaction pressure: ○, 200 mm Hg; □, 94 mm Hg.



Termination

For the derivation of an expression for the overall order, all possible combination reactions were considered, including radical combination and cross-combination reactions. Of these the following are the possible radical combination reactions

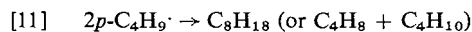
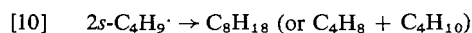


Table I lists the kinetic parameter ratios for elementary reactions involved in the above mechanism, with the exception of parameters for reactions [7] and [12].

Since most radical combination reactions have zero or very low activation energies, the values $E_i - \frac{1}{2}E_j$ in Table I are approximately equal to E_i .

In the following discussion it will be assumed that (i) the fundamental hypothesis of Bodenstein, that the intermediate products of the reac-

tion are of almost stationary concentration, is valid and (ii) the chain lengths involved are large.

Based on the proposed mechanism, a relationship between reaction products and rates may be established

$$([C_2H_4]/[C_2H_6]) - 1 = r_6/r_4$$

where r_i denotes the rate of reaction [i]. Above approximately 420 °C, the yield of ethylene is higher than the yield of ethane, thus reaction [6] has an appreciable rate. It is apparent from Fig. 2 that at lower temperatures the yields of ethane and ethylene are practically equivalent, and thus the rate of reaction [6] is negligible relative to the rate of reaction [4]. The temperature dependence of the relative rates of reactions [4] and [6] is mainly due to the difference in their activation energies (approximately 27.6 kcal).

Reactions [3] and [5] and reactions [2] and [4] are consecutive. Either one of these reaction pairs can complete a chain cycle converting a molecule of butane to products. Due to the large chain length, the rates of reactions [3] and [5] are approximately equal. The relative steady-state concentration of methyl and secondary butyl radicals is then dependent on the value of $k_3/k_5[C_4H_{10}]$. Above approximately 400 °C, $k_3 \gg k_5[C_4H_{10}]$ and therefore $[CH_3\cdot] \gg [s\text{-}C_4H_9\cdot]$. Similarly, $k_2 \gg (k_4[C_4H_{10}] \text{ or } k_6[C_4H_{10}]^e)$ and therefore $[C_2H_5\cdot] \gg [p\text{-}C_4H_9\cdot]$.

The above relative radical concentrations are

²The second term is introduced to represent the pressure dependence of this reaction, "e" is a stoichiometric coefficient, where $0 < e < 1$.

TABLE I
Kinetic parameters for the ratios of elementary reactions

Reaction		Frequency factor* $A_i/A_j^{1/2}$	Activation energy $E_i - \frac{1}{2}E_j$ (kcal/mole)	Reference
<i>i</i>	<i>j</i>			
2	11	7.94×10^6	28.7	Morganroth and Calvert (6)
3	10	1.31×10^8	32.6	Lin and Laidler (7)
4	9	2.45×10^4	10.4	Boddy and Steacie (8)
5	8	1.56×10^4	8.3	Trotman-Dickenson, Birchard, and Steacie (9)
6	9	8.5×10^6 †	38.0†	Lin and Back (10)

*In units of $\text{cc}^{1/2} \text{mole}^{-1/2} \text{s}^{-1/2}$ or $\text{cc}^{-1/2} \text{mole}^{1/2} \text{s}^{-1/2}$.

†First order region, at high pressures, extrapolated value.

pressure dependent. A higher pressure produces a higher butyl radical concentration relative to that of the methyl or ethyl radicals.

Since $E_3 > E_5$, then, as the temperature is lowered the value of $k_3/k_5[\text{C}_4\text{H}_{10}]$ decreases, resulting in an increased concentration of secondary butyl radicals relative to the concentration of the methyl radicals. A similar argument applies to the relationship between primary butyl and ethyl radicals. Thus, at lower temperatures and higher pressures butyl radicals become the main chain terminators.

The rates of reactions [4] and [5] are pressure dependent since *n*-butane is one of the reactants. The rates of reactions [2] and [3] are pressure independent. A higher pressure, therefore, produces a higher butyl radical concentration relative to that of the methyl or ethyl radicals.

In the previous recent publication already mentioned (3), an equation was developed to predict the reaction order for the pyrolysis of *n*-butane

$$\text{[II] Order} = \frac{\sum_{m=8}^{12} \sum_{n=8}^{12} (F_m + F_n)(r_m r_n)^{1/2}}{\sum_{m=8}^{12} \sum_{n=8}^{12} (r_m r_n)^{1/2}}$$

where values of *m*, *n*, F_m , and F_n are as given below.

Radical	<i>m</i> or <i>n</i>	$2(F_{m \text{ or } n})$
Methyl	8	1.5
Ethyl	9	$0.5 + u$
<i>s</i> -Butyl	10	0.5
<i>p</i> -Butyl	11	0.5
Hydrogen	12	$1.5 + u - e$

and

$r_{m \text{ or } n}$ = rate of reaction *m* or *n*

$$u = \frac{k_4[\text{C}_4\text{H}_{10}] + ek_6[\text{C}_4\text{H}_{10}]^e}{k_4[\text{C}_4\text{H}_{10}] + k_6[\text{C}_4\text{H}_{10}]^e}$$

$$0 < e < 1 \text{ and } 0 < u < 1$$

It was also shown that equations such as [II]

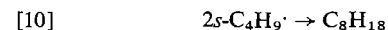
for the overall order may be expressed in terms of the kinetic parameters of the propagation reactions; in this case, they are the parameters listed in Table I, and eq. [I] represents the product distribution³.

Such an equation involving the kinetic parameters of the propagation reactions has been used for the prediction of the pressure and temperature dependence of the overall order of the pyrolysis of *n*-butane.

Equation [II] indicates that when reactions [10] or [11] predominate, the overall order is 0.5. When reaction [8] predominates, the overall order is 1.5, and when reaction [9] predominates it is between 0.5 and 1.5 (approximately 1.35 (3)).

The solid curve in Fig. 5 is a calculated one, assuming the predominance of reaction [8] over reaction [9] (at higher temperatures). The apparent difference between the experimental results and the calculated curve is most likely due to the uncertainties in the values of the kinetic parameters used in the calculations. The same equation was also used for the calculation of the log (rate) vs. log (pressure) curve shown in Fig. 4 along with the experimental points.

Lin and Laidler (7) studied the methyl radical initiated decomposition of *n*-butane in the 260–340 °C temperature region. They analyzed for the octanes which would be expected to be formed by the recombination of butyl radicals. Since 3,4-dimethylhexane was identified and *n*-octane was absent, it was indicated that



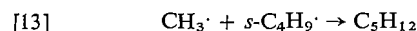
³Activation energies and frequency factors involved in the computation of $k_7/k_{12}^{1/2}$ are not listed in Table I and were not used in the calculation of the overall order, since reaction [12] is in its third-order region. The value of $k_7/k_{12}^{1/2}$ enters only into the calculation of r_{12} in eq. [II]. Since the rate of reaction [12] is much smaller than the rate of other chain-termination reactions, the value of r_{12} in eq. [II] may be assumed to be 0.

was the major chain-termination reaction. Calculations also indicate that the rate of reaction [10] is expected to be approximately 2 orders of magnitude larger than the rate of reaction [11].

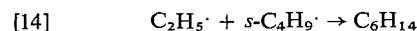
Chain-termination Mechanisms

In the previous publication (3), it was pointed out that the nature of the chain-termination mechanism at temperatures above 400 °C is still subject to considerable controversy. Either reaction [8] or reaction [9] may predominate.

In Fig. 5 it may be observed that at approximately 340 °C and 150 mm Hg the overall order is 1.0. Under these conditions the rate of the radical cross-combination reaction



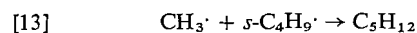
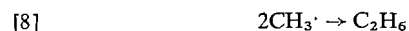
or



should become as important as the sum of the rates of the recombination reactions of the participating radicals.

The relative concentrations of C₅ and C₆ minor products of the sensitized decomposition of *n*-butane at 340 °C should reveal the relative concentrations of methyl and ethyl radicals, thereby providing useful information about the high temperature chain-termination mechanism.

Based on the results of this investigation, it may be concluded that reaction [10] predominates at temperatures below about 320 °C. At temperatures between 320 and 400 °C, both the high and the low temperature mechanism plus the cross-combination reaction of the 2 radicals involved is operative. Thus, assuming that reaction [8] is dominant at temperatures above 400 °C, the following chain-termination mechanism would apply to the 320–400 °C range



Conclusions

Organic radical decomposition reactions such

as reactions [2], [3], and [6] generally have a higher activation energy than radical exchange reactions like reactions [4] and [5]. At high temperatures, the small radicals are present at the highest concentrations and are thus the predominant chain terminators. As the temperature is lowered and the pressure increased, the larger radicals become more important as chain terminators. In a study of the pyrolysis of propane at 440 °C, Leathard and Purnell (11) observed an order change similar to the one described here. A likely reason for the apparent lack of other evidence is that order changes occur in a yet unexplored temperature region, where the reaction rate is extremely low. Extension of pyrolytic reaction studies to lower temperatures and moderately high pressures may reveal that many other organic, free-radical chain reactions can undergo a change in overall reaction order resulting from a change in the termination mechanism.

Acknowledgments

The authors wish to thank the National Research Council of Canada for financial assistance under Grant No. A1637 and the Spruce Falls Power and Paper Company for a fellowship to one of them (J.T.). They are also grateful to Mr. S. R. Rao for many stimulating discussions.

1. J. H. PURNELL and C. P. QUINN. *Proc. Roy. Soc. Ser. A*, **270**, 267 (1962).
2. N. H. SAGERT and K. J. LAIDLER. *Can. J. Chem.* **41**, 838 (1963).
3. J. TOROK and S. SANDLER. *Can. J. Chem.* **47**, 2707 (1969).
4. E. STEINMETZ, K. W. LANGE, and K. K.-G. SCHMITZ. *Chem. Ing. Tech.* **36**, 1103 (1964).
5. J. H. PURNELL and C. P. QUINN. *J. Chem. Soc.* 4128 (1961).
6. W. E. MORGANROTH and J. G. CALVERT. *J. Amer. Chem. Soc.* **88**, 5387 (1966).
7. M. C. LIN and K. J. LAIDLER. *Can. J. Chem.* **45**, 1315 (1967).
8. P. J. BODDY and E. W. R. STEACIE. *Can. J. Chem.* **38**, 1576 (1960).
9. A. F. TROTMAN-DICKENSON, J. R. BIRCHARD, and E. W. R. STEACIE. *J. Chem. Phys.* **19**, 163 (1951).
10. M. C. LIN and M. H. BACK. *Can. J. Chem.* **44**, 2357 (1966).
11. D. A. LEATHARD and J. H. PURNELL. *Proc. Roy. Soc. Ser. A*, **306**, 553 (1968).